Life Sciences 258 (2020) 118232

Contents lists available at ScienceDirect

Life Sciences

journal homepage: www.elsevier.com/locate/lifescie

Epigallocatechin-3-gallate mobilizes intracellular Ca^{2+} in prostate cancer cells through combined Ca^{2+} entry and Ca^{2+}-induced Ca^{2+} release

Carla Marchetti[a,*], Paola Gavazzo[a], Bruno Burlando[a,b]

[a] Istituto di Biofisica, Consiglio Nazionale delle Ricerche, via De Marini 6, 16149 Genova, Italy
[b] Dipartimento di Farmacia, Università di Genova, Viale Benedetto XV, 3 16132 Genova, Italy

ARTICLE INFO

Keywords:
Androgen-resistant prostate cancer cells
PC3 cells
DU145 cells
Green tea
Fura2
SH oxidation
Cytotoxicity
Ca^{2+}-induced Ca^{2+} release
ATP-induced Ca^{2+} release

ABSTRACT

Aims: To elucidate the mechanism by which (−)-epigallocatechin-3-gallate (EGCG) mediates intracellular Ca^{2+} increase in androgen-independent prostate cancer (PCa) cells.
Main methods: Following exposure to different doses of EGCG, viability of DU145 and PC3 PCa cells was evaluated by MTT assay and the intracellular Ca^{2+} dynamics by the fluorescent Ca^{2+} chelator Fura-2. The expression of different channels was investigated by qPCR analysis and sulfhydryl bonds by Ellman's assay.
Key findings: EGCG inhibited DU145 and PC3 proliferation with IC_{50} = 46 and 56 μM, respectively, and induced dose-dependent peaks of internal Ca^{2+} that were dependent on extracellular Ca^{2+}. The expression of TRPC4 and TRPC6 channels was revealed by qPCR in PC3 cells, but lack of effect by modulators and blockers ruled out an exclusive role for these, as well as for voltage-dependent T-type Ca^{2+} channels. Application of dithiothreitol and catalase and sulfhydryl (SH) measurements showed that EGCG-induced Ca^{2+} rise depends on SH oxidation, while the effect of EGTA, dantrolene, and the PLC inhibitor U73122 suggested that EGCG-induced Ca^{2+} influx acts as a trigger for Ca^{2+}-induced Ca^{2+} release, involving both ryanodine and IP_3 receptors. Different from EGCG, ATP caused a rapid Ca^{2+} increase, which was independent of external Ca^{2+}, but sensitive to U73122.
Significance: EGCG induces an internal Ca^{2+} increase in PCa cells by a multi-step mechanism. As dysregulation of cytosolic Ca^{2+} is directly linked to apoptosis in PCa cells, these data confirm the possibility of using EGCG as a synergistic adjuvant in combined therapies for recalcitrant malignancies like androgen-independent PCa.

1. Introduction

Prostate cancer (PCa), especially its androgen-independent form, is one of the commonest bad-prognosis malignancies worldwide. Given unsatisfactory outcome and adverse effects of treatments for androgen-independent PCa, biomedical attention is focused on the search for new therapies [53]. A followed strategy consists in considering possible preventive factors from lifestyle and diet. Epidemiologic evidence suggested a negative correlation between PCa incidence and green tea consumption in Asian countries, indicating a possible effect of the drink or of its active constituents for preventive or curative purposes, although data from observational studies are still not conclusive [1,2].

In most studies, the alleged health benefits of green tea has been associated to the activity of the major active compound, (-)-epigallocatechin-3-gallate (EGCG), a flavonoid esterified with gallic acid. EGCG has a long and distinguishable pedigree in cellular and molecular studies, many of which aimed at disclosing therapeutic targets [3]. In particular, EGCG was shown to cause cytotoxicity to cancer cell cultures at doses that are virtually harmless in tissue paired normal cells [4-6].

Intracellular Ca^{2+} is known to play an essential role in cancer development, while the cell Ca^{2+} mobilizing machinery often shows differences in cancer cells with respect to normal counterparts [7]. EGCG directly interacts with proteins and phospholipids in the plasma membrane and the intracellular Ca^{2+} elevation that is revealed at moderately high doses is likely to be one of the first steps of its action [8]. EGCG has been shown to induce Ca^{2+} influx *via* non-selective cation channels and voltage-operated Ca^{2+} channels in smooth muscle cells [9], and $O_2^{\bullet -}$-regulated Ca^{2+} channels in mast cells [10]. We have previously found that EGCG causes a reduction of viability by affecting T type Ca^{2+} channel activity in breast [11] and mesothelioma cancer cells [12]. Following this line of evidence, we have correlated dose-dependent effects of EGCG on cell viability with the Ca^{2+} dynamics in two androgen-insensitive human prostate carcinoma cell lines DU145 and PC3 PCa cells. By using various Ca^{2+} channel inhibitors and modulators of Ca^{2+} and redox cell signaling, we have tried to elucidate EGCG mechanism of action, which involves a multiplicity of Ca^{2+}

* Corresponding author.
E-mail address: marchetti@ge.ibf.cnr.it (C. Marchetti).

https://doi.org/10.1016/j.lfs.2020.118232
Received 19 May 2020; Received in revised form 31 July 2020; Accepted 5 August 2020
Available online 08 August 2020

mobilizing mechanisms, including cell membrane channels and intracellular Ca^{2+} release.

2. Material and methods

2.1. Chemicals

(−)-Epigallocatechin-3-gallate (EGCG) was purchased from Cayman Chemical Co. (Ann Arbor, MI, USA). All other reagents and analytical grade chemicals were purchased from Merck Life Science (Sigma-Aldrich, Milano, Italy), unless otherwise specified.

2.2. Cell culture and viability assay

In vitro experiments were carried out using the metastatic prostate cancer cell lines PC3 and DU145 [13]. Cells were obtained from the Genoa Tissue Bank (San Martino Hospital, Genova, Italy), and grown in RPMI medium, supplemented with 10% foetal bovine serum at 37 °C, in a 5% CO_2, fully humidified atmosphere.

Cell viability was determined by the MTT assay. Cells were settled in 96-well plates for 24 h and exposed to various agents for 24 or 48 h as specified. After that time, cells were incubated with 3-(4,5 Dimethylthiazol-2-yl)-2,5-diphenyltetrazolium salt (MTT, 0.5 mg/ml) added to the cell culture medium without serum for 3 h at 37 °C, treated with a solution of 1 N HCl–isopropanol (1:24, v/v) and mixed to dissolve the dark-blue formazan crystals formed. After a few minutes at room temperature, the plates were read at 570 nm in a VMax microplate reader (Molecular Devices, Sunyvale, CA).

2.3. Intracellular Ca^{2+} measurements

Cytosolic free Ca^{2+} concentration ($[Ca^{2+}]_i$) was measured using a microspectrophotometry fluorescence ratio setup equipped with a perfusion system, as previously described [14]. Cells were incubated with 5 μm Fura-2-acetoxymethyl ester (Fura-2-AM, Thermo Fisher Scientific) in a physiological saline (see below), at 37 °C for 40 min, washed and mounted on the stage of an inverted microscope (Axiovert Zeiss, Germany), where they were continually superfused with different solutions. Cells were illuminated by a xenon lamp through a wavelength selector monochromator; emission was observed through an X40 quartz objective and recorded by a photomultiplier. The ratio E340/E380 was calculated every 40 msec to acquire a time-dependent, internal Ca^{2+} sensitive signal. At the end of each experiment, cells were incubated with 2 μM ionomycin in 1 mM Ca^{2+} until the ratio reached a maximum value (R_{max}), then 10 mM ethylene glycol-bis(2-aminoethylether)-N,N,N′,N′-tetraacetic acid (EGTA) was applied until the ratio reached a minimum value (R_{min}). Finally, $MnCl_2$ (5 mM) was added to the bath to quench the Fura-2 fluorescence and determine the background fluorescence values. The fluorescence emissions relative to each excitation wavelength (E340 and E380 respectively) were corrected for this background signal before ratio R = E340/E380 determination. Internal Ca^{2+} was calculated according to the Grynkiewicz equation [15].

The physiological standard bath solution contained (in mM): NaCl 140, KCl 5.4, $CaCl_2$ 1.0, $MgCl_2$ 1.0, 4-(2-hydroxyethyl)-1-piperazineethanesulfonic acid (HEPES) 10, and glucose 10. The pH was adjusted at 7.4 with NaOH. The Ca^{2+}-free solution had the same composition with 0 $CaCl_2$ added, 4 $MgCl_2$ and 2 EGTA.

2.4. Real-time qPCR analysis

Total RNA from PC3 cultured cells was extracted using Aurum Total RNA Mini Kit (Bio-Rad, Hercules, CA, USA) according to manufacturer's instructions. Two micrograms of total RNA were retrotranscribed to cDNA using RNAse H+ MMLV reverse transcriptase and including in the reaction both random primers and oligo(dT) primers (iScript Advanced cDNA Synthesis Kit for RT-qPCR, Bio-Rad). In order to assess the expression of channel genes, cDNA was amplified using SYBR-Green dye (SsoAdvanced Universal SYBR Green Supermix, Bio-Rad) and CFX Connect Instrument (Bio-Rad). No template control (NTC), no primer control (NPC), no reverse transcription control (NAC), a reaction without reverse transcriptase, were included in the qPCR reactions to exclude genomic DNA contamination and the presence of primer dimers. Actin (*ACTB*) was used as an internal control with primer forward *5'ctggaacggtgaaggtgaca* and reverse *5'aagggacttcctgtaacaat*. PrimePCR™ SYBR green ® Assays from BIORAD were used for TRPV6, TRPC4and TRPC5 genes (qHsaCED0046278, qHsaCED0036540, and qHsaCID0017182, respectively), whereas for TRPC6 primers forward 5'*tggttacgttctttatggagtc* and reverse 5'*cacatcagcgtcatcctca* were as in [52]. The reaction conditions were: activation 95 °C 2 min; 39 cycles composed of denaturation 95 °C 5 s, annealing/extension 60 °C 30 s; melting curve 65–95 °C (0.5 °C increments) 5 s/step.

2.5. Estimation of free thiol groups

Free thiol groups were determined by Ellman's method [16]. Ellman's reagent (5,5′-dithio-*bis*-(2-nitrobenzoic acid), DTNB) was purchased from Thermo Scientific (Rockford, IL USA). Cells were grown in 6-well plates and incubated for 5 min with either dithiothreitol (DTT) 1 mM, EGCG 100 μM, both or no additions in standard physiological saline. Cells were washed 3 times with PBS without divalent cations (PBS^-) and set in PBS^- containing 0.02% ethylenediaminetetraacetic acid (EDTA) for 5 min. Then they were gently scraped from the wells, transferred in tubes and centrifuged at 1000 *g* for 3 min. Supernatant was rejected and cells were resuspended in PBS. The sample was then diluted with DTNB solution, according to the assay instructions, and absorbance was read at 420 nm in the VMax microplate reader.

The absorbance corresponding to the thiol concentration in the sample was calculated as

$$\Delta ABS_{420} = ((ABS_{420}{}^{*} - ABS_{420}{}^{b}) - (ABS_{420}{}^{0} - ABS_{420}{}^{b}))$$

where $ABS_{420}{}^{*}$ is the absorbance of the treated sample, $ABS_{420}{}^{0}$ is the control absorbance of untreated cells, and $ABS_{420}{}^{b}$ is blank absorbance.

2.6. Statistical analysis

Data were analysed using Sigma Plot software (Systat Software Inc.). Data are shown as mean ± sd for cytotoxicity assays and mean ± sem in all other experiments. Two-sample comparisons were evaluated by Student's *t*-test or Mann-Whitney Rank Sum test, as indicated by the software. Two-way ANOVA was carried out using R 3.2.3 software (www.r-project.org). Statistical difference was considered significant if $p < .05$ and indicated by * in the figures.

3. Results

3.1. Effect of EGCG on cell viability

EGCG was applied at different concentrations to DU145 and PC3 cells and inhibited proliferation with IC_{50} = 46 μM and 56 μM in DU145 cells and PC3 cells, respectively (Fig. 1).

3.2. Ca^{2+} dynamics induced by EGCG and ATP

Fura-2-loaded PC3 and DU145 cells were transiently exposed to EGCG and showed dose-dependent peaks of $[Ca^{2+}]_i$ (Fig. 2).

In both cell types, we compared the EGCG-induced Ca^{2+} rise with

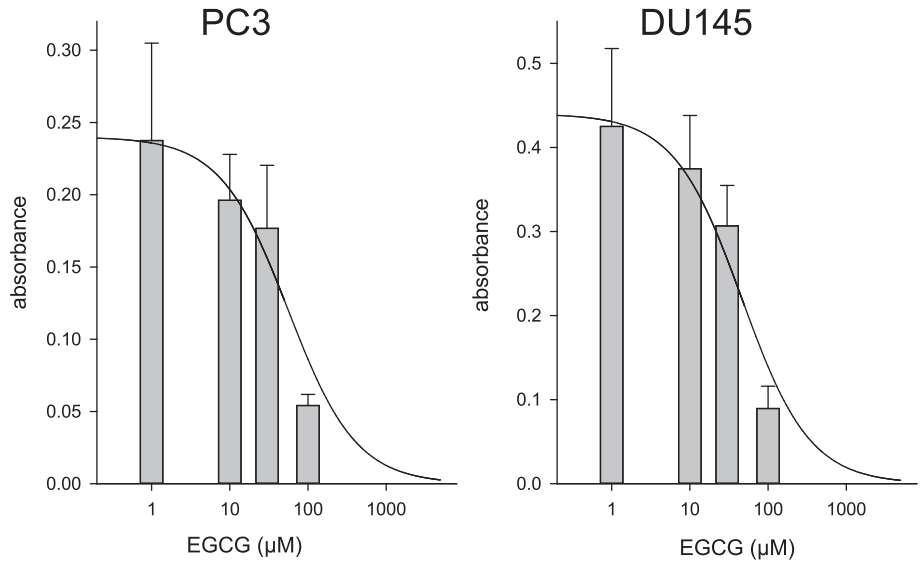

Fig. 1. Dose-response data of cell viability obtained with the MTT assay after exposure of PCa cells to EGCG for 48 h. Means ± s.d of percent MTT-formazan absorbance and logistic regression lines are shown. In PC3 cells, the IC_{50} is 56 μM and in DU145 cells, the IC_{50} is 46 μM.

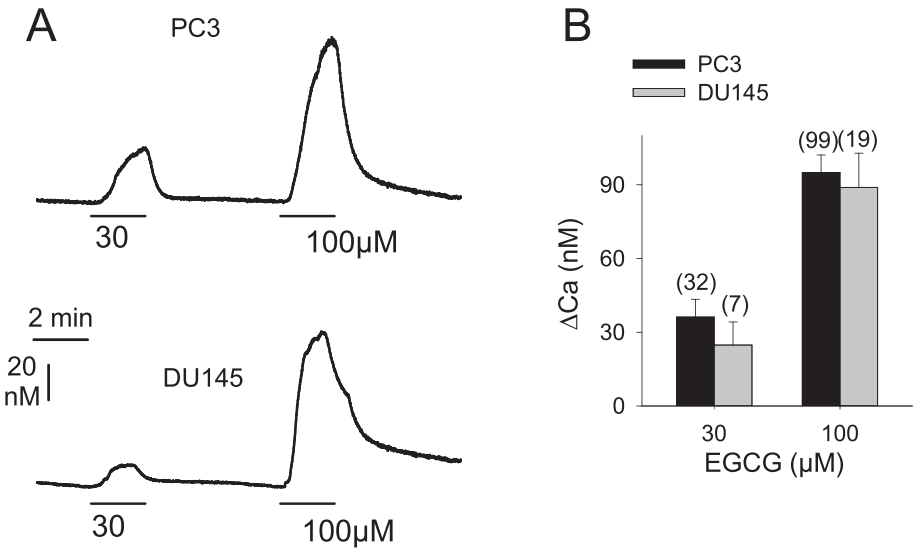

Fig. 2. $[Ca^{2+}]_i$ level in PCa cells loaded with Fura-2 and exposed to 30 and 100 M EGCG. (A) $[Ca^{2+}]_i$ spikes in Fura-2 loaded PC3 (above) and DU145 (below) cells following transient exposure to 30 and 100 μM EGCG. (B). Summary of the effects of 2 different doses of EGCG in DU145 and PC3 cells expressed as $\Delta Ca = [Ca^{2+}]_{i(EGCG)} - [Ca^{2+}]_{i(basal)}$. Number of experiments are indicated above each bar. Lines represent sem.

that triggered by ATP, which mobilizes Ca^{2+} from intracellular stores by activation of purinergic receptors [17,18]. Both cell types behaved very similarly, and no appreciable difference was apparent in any respect. As shown in Fig. 3, PC3 cells response to ATP was rapid, reached a peak in approximately 10 s of perfusion and it was quickly reversed. In contrast, the effect of EGCG developed more slowly, with delay of approximately 30 s from starting of perfusion, but was similarly reversible. In addition, the effect of ATP was completely independent of the external Ca^{2+} concentration, while that of EGCG was significantly reduced when the external concentration of Ca^{2+} was lowered by adding 2 mM EGTA.

Therefore, we investigated of a possible role played by external Ca^{2+} in the EGCG effect on cell viability. PC3 cells were exposed to different EGCG concentrations for 24 h in normal growth medium without serum or in the same medium containing 1 mM EGTA. Absorbance values were normalized to their respective control values to minimize the effect of EGTA on growth and attachment. Dose-response curves showed a significantly lower effect of EGCG in the absence of external Ca^{2+} (IC_{50} = 47 μM, 95% c.i. = 33–67, in the absence of EGTA; IC_{50} = 316 μM, 95% c.i. = 222–451, in the presence of EGTA) (Fig. 3C). By using non-normalized data, two-way ANOVA showed a significant interaction between EGTA and EGCG (F = 36.2, df = 3 and 1, respectively, $p < .01$), meaning that the effect of EGCG on cell viability was significantly different in the presence or absence of Ca^{2+}.

These observations show how, different from ATP, the effect of EGCG was dependent on Ca^{2+} entry, possibly through Ca^{2+} membrane channels. However, it was particularly interesting to compare two different protocols applied in Fura-2-loaded cells. In the first protocol (Fig. 3D1), cells were exposed to EGCG in a Ca-free EGTA-containing solution; the intracellular Ca^{2+} rise was initially quite small, but accelerated considerably when external Ca^{2+} was restored. This response was expected if EGCG response depends on external Ca^{2+}. In the second protocol (Fig. 3D2), cells were exposed to EGCG in the presence of Ca^{2+}, after 1 min external Ca^{2+} was removed and EGTA added for 2 min, and finally Ca^{2+} was restored. In this case, the Ca^{2+} rise proceeded quite unaltered. This behavior can be explained if external Ca^{2+} would act as a trigger for Ca^{2+} rise, whose origin is mainly from intracellular stores.

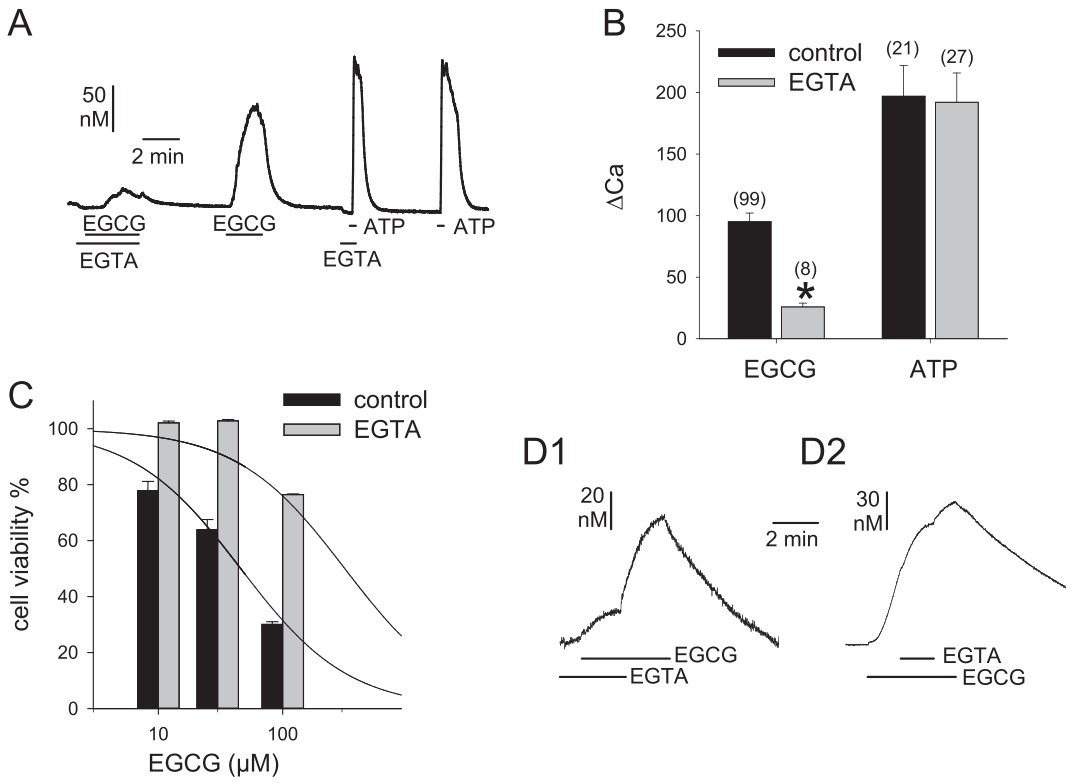

Fig. 3. Effect of the external Ca^{2+} concentration on the response to EGCG and ATP in PC3 cells. (A) - $[Ca^{2+}]_i$ spikes in Fura-2 loaded PC3 cells following transient exposure to 100 μM EGCG and to 10 μM ATP in 0 and 1 mM external Ca^{2+}. (B) – Summary of the $[Ca^{2+}]_i$ increase ($\Delta Ca = [Ca^{2+}]_{treated} - [Ca^{2+}]_{basal}$) following exposure to 100 μM EGCG and 10 μM ATP in 1 mM external Ca^{2+} and in 0 added Ca^{2+} and 2 mM EGTA respectively. Number of experiments are indicated above each bar. Lines represent sem. * indicates significantly different from control with $p < .05$. (C) Dose-response data of cell viability obtained as in Fig. 1, after exposure of PCa cells to EGCG for 24 h in a serum-free medium in control and in the presence of 1 mM EGTA. Absorbance values were normalized to their respective control values. IC_{50} was 47 μM without EGTA and 316 μM with EGTA. See text for details. (D) Effect of external Ca^{2+} on EGCG response following two different protocols. On the left (D1), EGCG (100 μM) is added in 0 Ca^{2+} + 2 mM EGTA solution and only a small increase of $[Ca^{2+}]_i$ is observed, as in the experiments shown in part (A) and (B) of the figure. Then external Ca^{2+} was restored to 1 mM and $[Ca^{2+}]_i$ started to rise more substantially. On the right (D2), EGCG was applied in the presence of 1 mM external Ca^{2+}; after 1 min Ca^{2+} was removed and EGTA (2 mM) added to the external solution for 2 min; finally 1 mM external Ca^{2+} was restored. With this protocol, repeated in other 2 similar experiments, $[Ca^{2+}]_i$ increased steadily, almost irrespective of the external Ca^{2+} concentration.

3.3. Search for possible Ca^{2+} channels involved in EGCG-induced Ca^{2+} rise

In the attempt to identify the Ca^{2+} channels involved, we tried different agents known to antagonize the diverse types of Ca^{2+} channels (Fig. 4). As previous work has suggested an involvement of T-type Ca^{2+} channel in EGCG-driven Ca^{2+} rise in different cancer cells [11,12], first we tried if Ni^{2+} (30 μM) was able to inhibit the response to EGCG (30–100 μM), but neither this ion nor the nonhydrolyzable analogue of mibefradil NNC 55-0396 ([19]; 5 μM, not shown) had appreciable effect on the EGCG response. The Ca^{2+} spike induced by 100 μM EGCG was likewise not significantly affected by 5 μM 4-methyl-'-[3,5-bis(trifluoromethyl)-1H-pyrazol-1-yl]-1,2,3-thiadiazole-5-carboxanilide (YM-58483), a blocker of store-operated Ca^{2+} entry [20]. Then we considered a possible contribution of nonselective, Ca^{2+} permeable cation channels of the TRP family [21], which have been suggested to play a role in prostate cancer cell proliferation [22], and are expressed in human prostate cancer DU145 and PC3 cells [23]. As these channels are differently modulated by trivalent cations, we tested the effect of Gd^{3+} (1 μM) and La^{3+} (2–10 μM), but neither antagonized the EGCG response. These data are summarized in Fig. 4.

Real-time qPCR analysis of mRNAs revealed the presence of Gd^{3+}-resistant TRPC6 [24], as well as TRPC4, but not TRPC5 genes, in our PC3 cultures (Fig. 5A). Expression of TRPV6 was also tested at least in 5 experiments, with three different couples of primers, one designed with Primer Blast, one chosen from literature [25], and the last the Bio-Rad Assay (see methods), but its presence was never detected.

Despite their expression, a predominant role of TRPC6 channels was ruled out because this channel is a store-independent diacylglycerol (DAG)-gated membrane channel [26,27] and the DAG analogue 1-oleoyl-2-acetyl-sn-glycerol (OAG) failed to enhance, but on the contrary contrasted, EGCG-driven Ca^{2+} rise (Fig. 5B, C).

The interference exerted by OAG on EGCG effect could suggest the involvement of TRPC4 channel, since this compound is known to prevent TRPC4 or TRPC5 activation [28]. However, in our system an essential role of TRPC4 channel is unlikely because ML204, a potent, and selective inhibitor [29] proved largely ineffective in preventing EGCG-induced Ca^{2+} rise (Fig. 5B, C). Therefore, a role of a particular TRPC channels could not be confirmed.

3.4. Role of redox mechanisms in the EGCG effect

The effect of EGCG was totally abolished in the presence of the reducing agent DTT (1 mM), which did not modify in any respect the

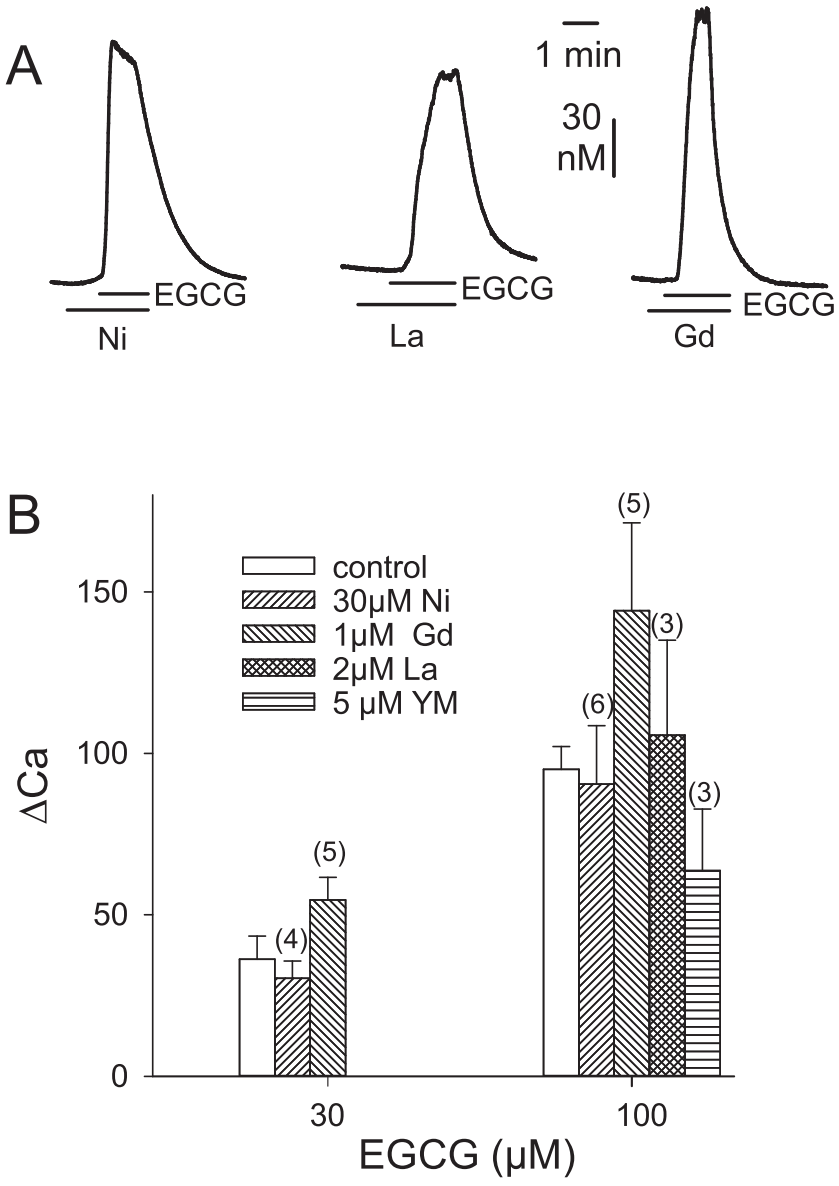

Fig. 4. Lack of effect of different modifiers on the response to EGCG in Fura-2 loaded PC3 cells. (A) $[Ca^{2+}]_i$ spikes following transient exposure to 100 μM EGCG in Fura-2 loaded PC3 cells in the presence of 30 μM Ni^{2+} (left trace), 2 μM La^{3+} (center trace) and 1 μM Gd^{3+} (right trace). All responses were not significantly different from that recorded in control conditions. (B) Summary of the effects of 30 and 100 μM EGCG in PC3 cells in control and in the presence of different agents. Control experiments are the same as in Figs. 2 and 3. Number of experiments are indicated above each bar. Lines represent sem. None of the conditions was significantly different from control.

response to ATP (Fig. 6A, C). This observation suggests that EGCG may cause oxidation of sulfhydryl bonds and this action may be prevented by DTT. To get further insight of this effect, we measured the sulfhydryl bonds in PC3 cells in different conditions by the Ellman method [16]. These experiments confirmed that EGCG can oxidize sulfhydryl bonds (Fig. 6D).

As EGCG was reported to cause H_2O_2 formation [11,30,31], we also examined the possibility that exogenous catalase (CAT), which scavenges H_2O_2, may interfere with EGCG effect. When cells were treated with CAT (500 U/ml) for up to 5 min before and during EGCG addition, frequently this resulted in a mild potentiation of the EGCG effect on Ca^{2+} (Fig. 6B, C), although the intracellular Ca^{2+} rise in the presence of CAT was not significantly different from that observed in control. Nevertheless this demonstrated that the intracellular Ca^{2+} increase is not mediated by H_2O_2 formation; instead CAT may facilitate EGCG-driven Ca^{2+} rise, possibly because it protects EGCG from oxidation, similarly to what has been previously observed with superoxide dismutase [32].

3.5. Role of Ca^{2+}-induced Ca^{2+} release

Because the role of a specific Ca^{2+} channel could not be identified, but external Ca^{2+} was important for the EGCG response, we hypothesized that this response was due to rather unspecific entry of small amounts of Ca^{2+} from outside, which trigger the Ca^{2+}-induced Ca^{2+} release (CICR) mechanism [33], as already reported with different agents in these cells [34,35]. In this respect, it appears significant that dantrolene, a well-known blocker of CICR [36], partially antagonized the Ca^{2+} rise driven by EGCG (Fig. 7A, C). Dantrolene is a known inhibitor of ryanodine receptors (RyRs), but some data argue that it could affect also inositol 1,4,5-tris-phosphate (IP_3) receptors [37]. To establish a possible involvement of these receptors, we used the aminosteroid

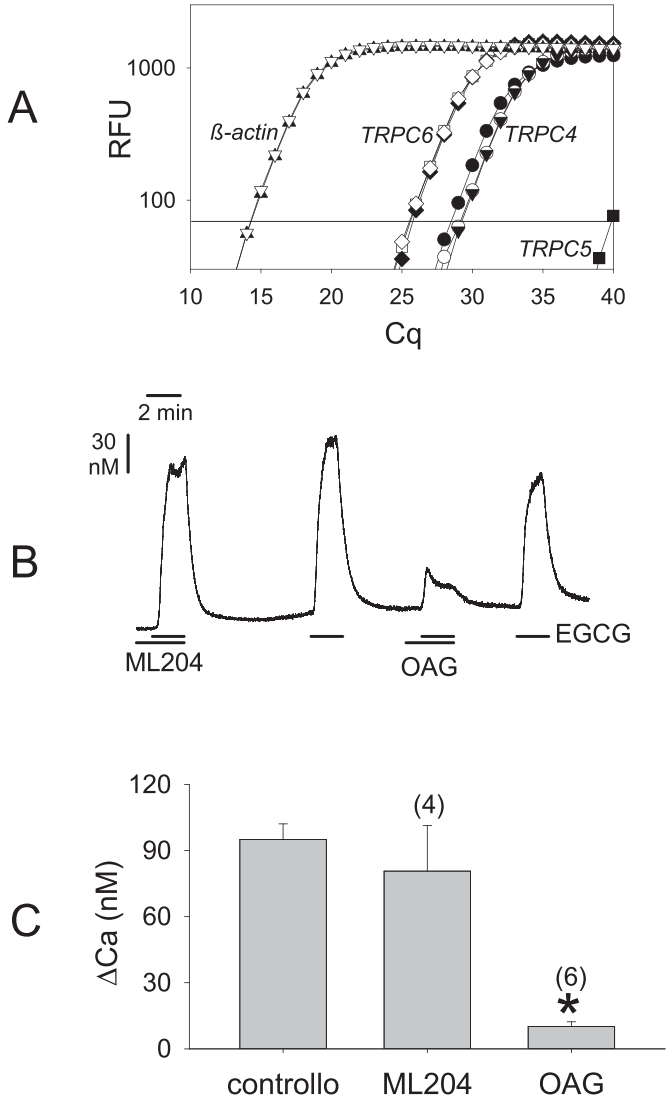

Fig. 5. (A) Real-time qPCR analysis of TRPC4, TRPC5 and TRPC6 cDNAs. The graph shows amplification plots of one PCR experiment representing the mean fluorescence increase during the run. The solid horizontal line represent the threshold line. Mean Cq values calculated from two different experiments with three replicates each were 15.49 ± 0.03 for β-actin; 30.33 ± 0.173 for TRPC4; N/A for TRPC5; 26.44 ± 0.045 for TRPC6.
(B) Time course of $[Ca^{2+}]_i$ in Fura-2 loaded PC3 cells following transient exposure to 100 μM EGCG in control and the presence of 5 μM ML204 and 40 μM OAG.
(C) Summary of the effects of 100 μM EGCG in PC3 cells in control and in the presence of 5 μM ML204 or 40 μM OAG. Lines represent sem. Number of experiments are indicated above each bar. * indicates $p < .05$ with respect to control.

U73122 (1-(6-((17β-3-methoxyestra-1,3,5(10)-trien-17-yl)amino) hexyl)-1*H*-pyrrole-2,5-dione), a potent inhibitor of phospholipase C (PLC) enzymes and IP_3-mediated Ca^{2+} release. U73122 (1 and 5 μM) completely abolished the Ca^{2+} peak following ATP application and antagonized significantly also that application of EGCG, confirming the involvement of PLC in both mechanisms (Fig. 7B, C). On the contrary, O-tricyclo[5.2.1.$0^{2,6}$]dec-9-yl dithiocarbonate (D609), a selective inhibitor of phosphatidylcholine (PC)-specific phospholipase C [38] did not antagonize EGCG effect, indicating that this PLC was not involved (Fig. 7C).

4. Discussion

Viability assays performed in this study confirmed cytotoxicity of EGCG on PCa cells. Our results are in quantitative agreement with previous data on the same cell lines [39] as well as tests on different cancer cells [4,11,12] and represent the logical premise for investigating the role of EGCG as a possible bioactive agent with pharmacological relevance against PCa. We wanted to characterize the first step of the functional interaction of EGCG with PCa cells, namely a dose-dependent internal Ca^{2+} elevation. It is well known that internal Ca^{2+} level is an important trigger of apoptosis in androgen-independent prostate cancer cells [40,41]. In PC3 cells, removal of external Ca^{2+} and supplement with EGTA largely prevented EGCG-driven Ca^{2+} elevation and significantly reduced the EGCG effect on cell viability, suggesting that the EGCG-driven Ca^{2+} rise was dependent on Ca^{2+} influx through an unidentified Ca^{2+} transport system. Although in apparent agreement with previous findings, more detailed investigation highlighted discrepancies with respect to former studies in different cells. In malignant mesothelioma [11] and breast cancer cells [12], EGCG was reported to open T-type Ca^{2+} channels, while in this study, the possibility of an involvement of these Ca^{2+} channels was ruled out by the failure of Ni^{2+} and of the specific T-type inhibitor NNC-55-0396 to block the EGCG-induced Ca^{2+} rise.

The involvement of a different Ca^{2+} channel was expected. It is very unlikely that voltage-dependent channels may play any role in these cells and therefore we addressed to Ca^{2+} channels that can be activated by diverse stimuli. As largely expressed in advanced prostate cancer, we first sought for a possible role of TRPV6 [42], but this channel was not detectable in our cells by RT-qPCR. The insensitivity to YM-58483, a blocker of store-operated Ca^{2+} entry [20] and to 1 μM Gd^{3+} would suggest the involvement of Gd^{3+}-resistant Ca^{2+} channel, belonging to the family of canonical transient receptor potential (TRPC; [21,24]). Based on previous data on prostate cancer and TRPC channels, we focused on two representatives of the two main subgroups TRPC2/3/6/7 and TRPC1/4/5, namely the TRPC6 and TRPC4 isoforms [43–45]. The expression of TRPC6 in these PC3 cells was confirmed by RT-qPCR, but OAG, a membrane-permeant analogue of DAG, failed to facilitate the response to EGCG and, opposite to this, caused a reversible decrease of this response. Because TRPC6 is store-independent DAG-gated membrane channel [27], its role is challenged by this observation. Similarly, also the expression of TRPC4 was confirmed by RT-qPCR, but the role of this channel was ruled out by failure of its ML204 selective inhibitor to abolish the EGCG effect.

So the sole contribution of a particular, fully identified, Ca^{2+} channel in the EGCG response is questionable because it was impossible to characterize a pharmacological profile that identify a single Ca^{2+} channel type.

Conversely, the action of EGCG appeared to be linked to the activation of PLC and involvement of CICR, possibly through sensitization of RyR [46]. The inhibition induced by U73122 was stronger than that obtained with dantrolene (Fig. 7), thus supporting the hypothesis of a CICR mechanism mainly sustained by IP_3-mediated intracellular Ca^{2+} release, but with an essential contribution of RyRs.

Therefore, all data concur to suggest that the effect of EGCG on cytosolic Ca^{2+} is a multiple step process. This process is initiated by a limited entry of Ca^{2+} from the outside, possibly through a mechanism involving different kinds of Ca^{2+} channels endowed with redox-sensitive sulfhydryls. The sensitivity to redox processes causes a specific and frequently uncontrolled opening of different kinds of Ca^{2+} channels

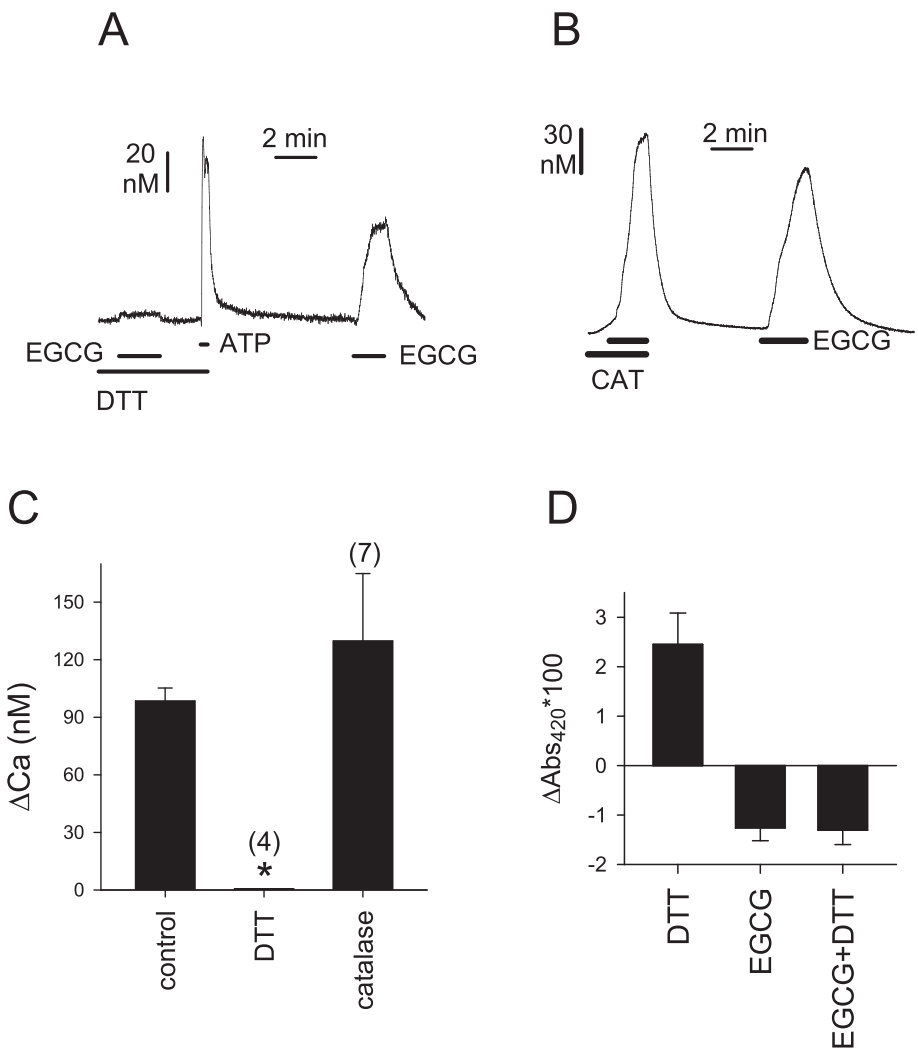

Fig. 6. Effect of DTT and catalase on the response to EGCG in Fura-2 loaded PC3 cells. (A) Time course of $[Ca^{2+}]_i$ in Fura-2 loaded PC3 cells following transient exposure to 100 μM EGCG and to 10 μM ATP in the presence of DTT (1 mM). The response to 100 μM EGCG is also shown after wash. (B) Time course of $[Ca^{2+}]_i$ in Fura-2 loaded PC3 cells following exposure to 100 μM EGCG with pretreatment and in the presence of catalase (500 U/ml) and after wash. (C) - Summary of the effects of 100 μM EGCG in PC3 cells in control and in the presence and after pretreatment with 1 mM DTT or 500 U/ml catalase. Number of experiments are indicated above each bar. Lines represent sem. * indicates $p < .05$ with respect to control. (D) Measure of sulfhydryl bonds in PC3 cells in different conditions by the Ellman method.

[47]. As EGCG effect was not antagonize by CAT, H_2O_2 formation is unlikely. On the contrary, our data argue that EGCG oxidizes sulfhydryls through direct binding, rather than through the intermediate of reactive oxygen species, consistent with the known ability of EGCG to covalently bind nucleophilic residues of proteins [48]. Subsequently, a moderate cytosolic Ca^{2+} rise would trigger a greater intracellular Ca^{2+} mobilization through a CICR mechanism. This latter would be sustained by an interplay of ryanodine and IP_3 receptors, similarly to what has been observed in rat female pain receptors and mouse granulosa cells [49,50].

Both these two hypothesized segments of the multi-step EGCG effect correspond to well-known mechanisms of Ca^{2+} dynamics [33]. This pathway of action can be generalized to other substances capable of sulfhydryls oxidation and depending on sensitivity of ER receptors and state of filling of ER stores. A similar mechanism initiated by a moderate Ca^{2+} influx was proposed and demonstrated to occur in PC3 cells in response to different modulators [34,35] and may be a generalized mechanism for Ca^{2+} dysregulation in these and other cancer cells.

The assumption of a multi-step process induced by EGCG is in agreement with induction of a delayed Ca^{2+} rise with respect to that of ATP. Our data indicate that ATP acts on PC3 cells through purinergic receptors [17] and PLC metabotropic process that is independent of extracellular Ca^{2+} and entirely dependent on intracellular Ca^{2+} release. This mechanism is much faster than that used by EGCG and involves only Ca^{2+} mobilization and intracellular Ca^{2+} channels.

Imbalance of cytosolic Ca^{2+} is directly linked to apoptosis in PCa cells [41], as well as in other cancer cell types [40]. Therefore, it is likely that the significant reduction of PCa cell viability induced by EGCG occurs through this kind of mechanism. With IC_{50} ranging between 20 and 100 μM (reviewed in [5]), EGCG cannot be directly competitive with standard anticancer drugs, but open the possibility for its use as a synergistic adjuvant in combined therapies [40,51]. This kind of strategy may be extremely important for recalcitrant malignancies, like androgen-independent PCa, in which maximum tolerated doses of conventional antitumor drugs, either alone or in combination, fail to produce resolutive outcome.

5. Conclusions

Our data show that EGCG induces an internal Ca^{2+} increase in PCa cells by a multi-step mechanism, initiated by oxidation of sulfhydryls on membrane Ca^{2+} transport proteins, followed by an enhanced Ca^{2+} leak from the outside and a more sustained CICR through RyRs, with an important contribution of IP_3-driven Ca^{2+} release from the endoplasmic reticulum. The requirement of a moderate Ca^{2+} entry for a basically intracellular mediated mechanism of Ca^{2+} release is likely to be typical of non-excitable cells. These data argue for the possible use of EGCG as a coadjuvant in the treatment of recalcitrant PCa, and in addition suggest that the alleged health benefit of green tea for cancer prevention and cure may be linked to synergistic intervention of different factors including internal Ca^{2+} dysregulation.

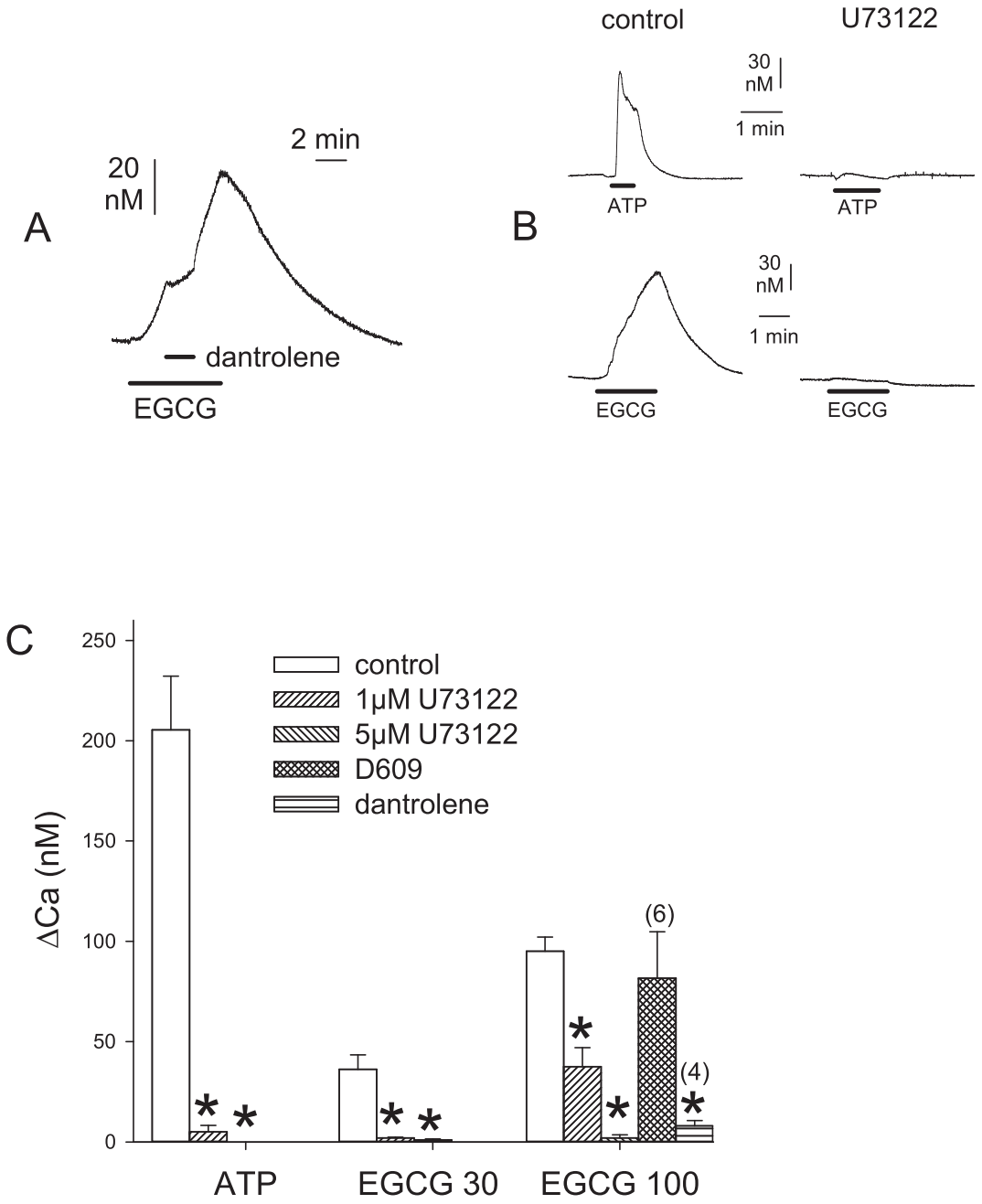

Fig. 7. Effect of internal Ca^{2+} modifiers on EGCG and ATP effect. (A) Time course of $[Ca^{2+}]_i$ in Fura-2 loaded PC3 cells following exposure to 100 μM EGCG and the transient application of dantrolene (10 μM). (B) Time course of $[Ca^{2+}]_i$ in Fura-2 loaded PC3 cells following transient exposure to 10 μM ATP or 100 μM EGCG in control and after pretreatment and in the presence of 5 μM U73122. (C) Summary of the effects of 10 μM ATP and 30 or 100 μM EGCG in PC3 cells in control and in the presence and after pretreatment with 1 and 5 μM U73122, and effect of 100 μM EGCG with 5 μM D609 or 10 μM dantrolene. Lines represent sem over 3 experiments with U73122 or number of experiments indicated above each bar. * indicates $p < .05$ with respect to control.

Declaration of competing interest

The authors declare no conflict of interest.

Acknowledgements

This work was supported by National Research Council of Italy (CNR, Rome). This research did not receive any specific grant from funding agencies in the public, commercial, or not-for-profit sectors.

References

[1] Filippini T, Malavolti M, Borrelli F, Izzo AA, Fairweather-Tait SJ, Horneber M, Vinceti M. (2020) Green tea (Camellia sinensis) for the prevention of cancer. Cochrane Database Syst. Rev. 2020; Issue 3. Art. No.: CD005004. doi:https://doi.org/10.1002/14651858.CD005004.pub3.

[2] J.M. Yuan, Cancer prevention by green tea: evidence from epidemiologic studies, Am. J. Clin. Nutr. 98 (6 Suppl) (2013) 1676S–1681S, https://doi.org/10.3945/ajcn.113.058271.

[3] B.N. Singh, S. Shankar, R.K. Srivastava, Green tea catechin, epigallocatechin-3-gallate (EGCG): mechanisms, perspectives and clinical applications, Biochem. Pharmacol. 82 (2011) 1807–1821, https://doi.org/10.1016/j.bcp.2011.07.093.

[4] J.H. Weisburg, D.B. Weissman, T. Sedaghat, H. Babich, In vitro cytotoxicity of epigallocatechin gallate and tea extracts to cancerous and normal cells from the

human oral cavity, Basic Clin Pharmacol Toxicol 95 (2004) 191–200, https://doi.org/10.1111/j.1742-7843.2004.pto_950407.x.
[5] R.Y. Gan, H.B. Li, Z.Q. Sui, H. Corke, Absorption, metabolism, anti-cancer effect and molecular targets of epigallocatechin gallate (EGCG): an updated review, Crit. Rev. Food Sci. Nutr. 58 (2018) 924–941, https://doi.org/10.1080/10408398.2016.1231168.
[6] M.A. Shammas, P. Neri, H. Koley, R.B. Batchu, R.C. Bertheau, V. Munshi, R. Prabhala, M. Mariateresa Fulciniti, Y.T. Tai, S.P. Treon, R.K. Goyal, K.C. Anderson, N.C. Munshi, Specific killing of multiple myeloma cells by (-)-epigallocatechin-3-gallate extracted from green tea: biologic activity and therapeutic implications, Blood 108 (8) (2006) 2804–2810, https://doi.org/10.1182/blood-2006-05-022814.
[7] G.R. Monteith, D. McAndrew, H.M. Faddy, S.J. Roberts-Thomson, Calcium and cancer: targeting Ca^{2+} transport, Nat. Rev. Cancer 7 (2007) 519–530, https://doi.org/10.1038/nrc2171.
[8] H. Kim, M.J. Quon, J. Kim, New insights into the mechanisms of polyphenols beyond antioxidant properties; lessons from the green tea polyphenol, epigallocatechin 3-gallate, Redox Biol. 2 (2014) 187–195, https://doi.org/10.1016/j.redox.2013.12.022.
[9] M. Campos-Toimil, F. Orallo, Effects of (-)-epigallocatechin-3-gallate in Ca2+ -permeable non-selective cation channels and voltage-operated Ca2+ channels in vascular smooth muscle cells, Life Sci. 80 (2007) 2147–2153.
[10] T. Inoue, Y. Suzuki, C. Ra, Epigallocatechin-3-gallate induces cytokine production in mast cells by stimulating an extracellular superoxide-mediated calcium influx, Biochem. Pharmacol. 82 (2011) 1930–1939, https://doi.org/10.1016/j.bcp.2011.09.011.
[11] E. Ranzato, S. Martinotti, V. Magnelli, B. Murer, S. Biffo, L. Mutti, B. Burlando, Epigallocatechin-3-gallate induces mesothelioma cell death via H2 O2 -dependent T-type Ca2+ channel opening, J. Cell. Mol. Med. 16 (2012) 2667–2678.
[12] E. Ranzato, V. Magnelli, S. Martinotti, Z. Waheed, S.M. Cain, T.P. Snutch, C. Marchetti, B. Burlando, Epigallocatechin-3-gallate elicits Ca^{2+} spike in MCF-7 breast cancer cells: essential role of Cav3.2 channels, Cell Calcium 56 (2014) 285–295, https://doi.org/10.1016/j.ceca.2014.09.002.
[13] A. van Bokhoven, M. Varella-Garcia, C. Korch, W.U. Johannes, E.E. Smith, H.L. Miller, S.K. Nordeen, G.J. Miller, M.S. Lucia, Molecular characterization of human prostate carcinoma cell lines, Prostate 57 (3) (2003) 205–225, https://doi.org/10.1002/pros.10290.
[14] C. Marchetti, S. Ribulla, V. Magnelli, M. Patrone, B. Burlando, Resveratrol induces intracellular Ca^{2+} rise via T-type Ca^{2+} channels in a mesothelioma cell line, Life Sci. 148 (2016) 125–131, https://doi.org/10.1016/j.lfs.2016.01.048.
[15] G. Grynkiewicz, M. Poenie, R.Y. Tsien, A new generation of Ca2+ indicators with greatly improved fluorescence properties, J. Biol. Chem. 260 (1985) 3440–3450.
[16] P.W. Riddles, R.L. Blakeley, B. Zerner, Reassessment of Ellman's reagent, Methods Enzymol. 91 (1983) 49–60, https://doi.org/10.1016/s0076-6879(83)91010-8.
[17] R. Janssens, J.M. Boeynaems, Effects of extracellular nucleotides and nucleosides on prostate carcinoma cells, Br. J. Pharmacol. 132 (2001) 536–546, https://doi.org/10.1038/sj.bjp.0703833.
[18] W.J. Wasilenko, J. Cooper, A.J. Palad, K.D. Somers, P.F. Blackmore, J.S. Rhim, G.L. Wright Jr., P.F. Schellhammer, Calcium signaling in prostate cancer cells: evidence for multiple receptors and enhanced sensitivity to bombesin/GRP, Prostate 30 (3) (1997) 167–173, https://doi.org/10.1002/(sici)1097-0045(19970215)30:3<167::aid-pros4>3.0.co;2-j.
[19] L. Huang, B.M. Keyser, T.M. Tagmose, J.B. Hansen, J.T. Taylor, H. Zhuang, M. Zhang, D.S. Ragsdale, M. Li, NNC 55-0396 [(1S,2S)-2-(2-(N-[(3-benzimidazol-2-yl)propyl]-N-methylamino)ethyl)-6-fluoro-1,2, 3,4-tetrahydro-1-isopropyl-2-naphtyl cyclo propanecarboxylate dihydrochloride]: a new selective inhibitor of T-type calcium channels, J. Pharmacol. Exp. Ther. 309 (2004) 193–199, https://doi.org/10.1124/jpet.103.060814.
[20] J. Ishikawa, K. Ohga, T. Yoshino, R. Takezawa, A. Ichikawa, H. Kubota, T. Yamada, A pyrazole derivative, YM-58483, potently inhibits store-operated sustained Ca2+ influx and IL-2 production in T lymphocytes, J. Immunol. 170 (9) (2003) 4441–4449, https://doi.org/10.4049/jimmunol.170.9.4441.
[21] L. Birnbaumer, The TRPC class of ion channels: a critical review of their roles in slow, sustained increases in intracellular Ca(2+) concentrations, Annu. Rev. Pharmacol. Toxicol. 49 (2009) 395–426, https://doi.org/10.1146/annurev.pharmtox.48.113006.094928.
[22] D. Gkika, N. Prevarskaya, TRP channels in prostate cancer: the good, the bad and the ugly? Asian J Androl 13 (5) (2011) 673–676, https://doi.org/10.1038/aja.2011.18.
[23] Y. Wang, D. Yue, K. Li, Y.L. Liu, C.S. Ren, P. Wang, The role of TRPC6 in HGF-induced cell proliferation of human prostate cancer DU145 and PC3 cells, Asian J Androl 12 (6) (2010) 841–852, https://doi.org/10.1038/aja.2010.85.
[24] Y. Liao, C. Erxleben, J. Abramowitz, V. Flockerzi, M.X. Zhu, D.L. Armstrong, L. Birnbaumer, Functional interactions among Orai1, TRPCs, and STIM1 suggest a STIM-regulated heteromeric Orai/TRPC model for SOCE/Icrac channels, Proc. Natl. Acad. Sci. U. S. A. 105 (8) (2008) 2895–2900, https://doi.org/10.1073/pnas.0712288105.
[25] Y. Jiang, H. Gou, J. Zhu, S. Tian, L. Yu, Lidocaine inhibits the invasion and migration of TRPV6-expressing cancer cells by TRPV6 downregulation, Oncol. Lett. 12 (2) (2016) 1164–1170, https://doi.org/10.3892/ol.2016.4709.
[26] T. Hofmann, A.G. Obukhov, M. Schaefer, C. Harteneck, T. Gudermann, G. Schultz, Direct activation of human TRPC6 and TRPC3 channels by diacylglycerol, Nature 397 (6716) (1999) 259–263, https://doi.org/10.1038/16711.
[27] S. Thebault, M. Flourakis, K. Vanoverberghe, F. Vandermoere, M. Roudbaraki, V. Lehen'kyi, C. Slomianny, B. Beck, P. Mariot, J.L. Bonnal, B. Mauroy, Y. Shuba, T. Capiod, R. Skryma, N. Prevarskaya, Differential role of transient receptor potential channels in Ca^{2+} entry and proliferation of prostate cancer epithelial cells, Cancer Res. 66 (4) (2006) 2038–2047, https://doi.org/10.1158/0008-5472.CAN-05-0376.
[28] K. Venkatachalam, F. Zheng, Donald L. Gill, Regulation of canonical transient receptor potential (TRPC) channel function by diacylglycerol and protein kinase C, J. Biol. Chem. 278 (31) (2003) 29031–29040, https://doi.org/10.1074/jbc.M302751200.
[29] M. Miller, J. Shi, Y. Zhu, M. Kustov, J.B. Tian, A. Stevens, M. Wu, J. Xu, S. Long, P. Yang, A.V. Zholos, J.M. Salovich, C.D. Weaver, C.R. Hopkins, C.W. Lindsley, O. McManus, M. Li, M.X. Zhu, Identification of ML204, a novel potent antagonist that selectively modulates native TRPC4/C5 ion channels, J. Biol. Chem. 286 (2011) 33436–33446, https://doi.org/10.1074/jbc.M111.274167.
[30] J. Hong, H. Lu, X. Meng, J.H. Ryu, Y. Hara, C.S. Yang, Stability, cellular uptake, biotransformation, and efflux of tea polyphenol (-)-epigallocatechin-3-gallate in HT-29 human colon adenocarcinoma cells, Cancer Res. 62 (24) (2002) 7241–7246.
[31] T. Yamamoto, J. Lewis, J. Wataha, D. Dickinson, B. Singh, W.B. Bollag, E. Ueta, T. Osaki, M. Athar, G. Schuster, S. Hsu, Roles of catalase and hydrogen peroxide in green tea polyphenol-induced chemopreventive effects, J. Pharmacol. Exp. Ther. 308 (1) (2004) 317–323, https://doi.org/10.1124/jpet.103.058891.
[32] Z. Hou, S. Sang, H. You, M.J. Lee, J. Hong, K.V. Chin, C.S. Yang, Mechanism of action of (-)-epigallocatechin-3-gallate: auto-oxidation-dependent inactivation of epidermal growth factor receptor and direct effects on growth inhibition in human esophageal cancer KYSE 150 cells, Cancer Res. 65 (17) (2005) 8049–8056, https://doi.org/10.1158/0008-5472.CAN-05-0480.
[33] M.D. Bootman, M.J. Berridge, H.L. Roderick, Calcium signalling: more messengers, more channels, more complexity, Curr. Biol. 12 (16) (2002) R563–R565, https://doi.org/10.1016/s0960-9822(02)01055-2.
[34] T. Petrou, H.L. Olsen, C. Thrasivoulou, J.R. Masters, J.F. Ashmore, A. Ahmed, Intracellular calcium mobilization in response to ion channel regulators via a calcium-induced calcium release mechanism, J. Pharmacol. Exp. Ther. 360 (2) (2017) 378–387, https://doi.org/10.1124/jpet.116.236695.
[35] M. Reyes-Corral, N.M. Sørensen, C. Thrasivoulou, P. Dasgupta, J.F. Ashmore, A. Ahmed, Differential free intracellular calcium release by class II antiarrhythmics in cancer cell lines, J. Pharmacol. Exp. Ther. 369 (1) (2019) 152–162, https://doi.org/10.1111/j.1582-4934.2012.01584.x.
[36] F. Zhao, P. Li, S.R. Chen, C.F. Louis, B.R. Fruen, Dantrolene inhibition of ryanodine receptor Ca^{2+} release channels. Molecular mechanism and isoform selectivity, J. Biol. Chem. 276 (17) (2001) 13810–13816, https://doi.org/10.1074/jbc.M006104200.
[37] N. Ansari, H. Hadi-Alijanvand, M. Sabbaghian, M. Kiaei, F. Khodagholi, Interaction of 2-APB, dantrolene, and TDMT with IP3R and RyR modulates ER stress-induced programmed cell death I and II in neuron-like PC12 cells: an experimental and computational investigation, J. Biomol. Struct. Dyn. 32 (8) (2014) 1211–1230, https://doi.org/10.1080/07391102.2013.812520.
[38] R.M. Adibhatla, J.F. Hatcher, A. Gusain, Tricyclodecan-9-yl-xanthogenate (D609) mechanism of actions: a mini-review of literature, Neurochem. Res. 37 (4) (2012) 671–679, https://doi.org/10.1007/s11064-011-0659-z.
[39] D.S. Albrecht, E.A. Clubbs, M. Ferruzzi, J.A. Bomser, Epigallocatechin-3-gallate (EGCG) inhibits PC-3 prostate cancer cell proliferation via MEK-independent ERK1/2 activation, Chem. Biol. Interact. 171 (2008) 89–95, https://doi.org/10.1016/j.cbi.2007.09.001.
[40] S. Martinotti, E. Ranzato, M. Parodi, M. Vitale, B. Burlando, Combination of ascorbate/epigallocatechin-3-gallate/gemcitabine synergistically induces cell cycle deregulation and apoptosis in mesothelioma cells, Toxicol. Appl. Pharmacol. 2274 (2014) 35–41, https://doi.org/10.1016/j.taap.2013.10.025.
[41] N. Prevarskaya, R. Skryma, Y. Shuba, Ca^{2+} homeostasis in apoptotic resistance of prostate cancer cells, Biochem. Biophys. Res. Commun. 322 (4) (2004) 1326–1335, https://doi.org/10.1016/j.bbrc.2004.08.037.
[42] V. Lehen'kyi, M. Flourakis, R. Skryma, N. Prevarskaya, TRPV6 channel controls prostate cancer cell proliferation via Ca(2+)/NFAT-dependent pathways, Oncogene 26 (52) (2007) 7380–7385, https://doi.org/10.1038/sj.onc.1210545.
[43] J. Duan, J. Li, B. Zeng, G. Chen, X. Peng, Y. Zhang, J. Wang, D.E. Clapham, Z. Li, Zhang J (2018) Structure of the mouse TRPC4 ion channel, Nat. Commun. 9 (1) (2018) 3102, https://doi.org/10.1038/s41467-018-05247-9.
[44] M. Flourakis, N. Prevarskaya, Insights into Ca^{2+} homeostasis of advanced prostate cancer cells, Biochim. Biophys. Acta 1793 (6) (2009) 1105–1109, https://doi.org/10.1016/j.bbamcr.2009.01.009.
[45] S. Sharma, C.R. Hopkins, Review of transient receptor potential canonical (TRPC5) channel modulators and diseases, J. Med. Chem. 62 (17) (2019) 7589–7602, https://doi.org/10.1021/acs.jmedchem.8b01954.
[46] W. Feng, G. Cherednichenko, C.W. Ward, I.T. Padilla, E. Cabrales, J.R. Lopez, J.M. Eltit, P.D. Allen, I.N. Pessah, Green tea catechins are potent sensitizers of ryanodine receptor type 1 (RyR1), Biochem. Pharmacol. 80 (4) (2010) 512–521, https://doi.org/10.1016/j.bcp.2010.05.004.
[47] I. Bogeski, R. Kappl, C. Kummerow, R. Gulaboski, M. Hoth, B.A. Niemeyer, Redox regulation of calcium ion channels: chemical and physiological aspects, Cell Calcium 50 (5) (2011) 407–423, https://doi.org/10.1016/j.ceca.2011.07.006. 10.1016/j.ceca.2011.07.006.
[48] D. Cao, Y. Zhang, H. Zhang, L. Zhong, X. Qian, Systematic characterization of the covalent interactions between (-)-epigallocatechin gallate and peptides under physiological conditions by mass spectrometry, Rapid Commun. Mass Spectrom. 23 (8) (2009) 1147–1157, https://doi.org/10.1002/rcm.3985.
[49] V. Morales-Tlalpan, R.O. Arellano, M. Díaz-Muñoz, Interplay between ryanodine and IP3 receptors in ATP-stimulated mouse luteinized-granulosa cells, Cell Calcium 37 (2005) 203–213, https://doi.org/10.1016/j.ceca.2004.10.001.
[50] E.V. Khomula, L.F. Ferrari, D. Araldi, J.D. Levine, Sexual dimorphism in a reciprocal

interaction of ryanodine and IP 3 receptors in the induction of hyperalgesic priming, J. Neurosci. 37 (8) (2017) 2032–2044, https://doi.org/10.1523/JNEUROSCI.2911-16.2017.
[51] V. Volta, E. Ranzato, S. Martinotti, S. Gallo, M.V. Russo, L. Mutti, S. Biffo, B. Burlando, Preclinical demonstration of synergistic active nutrients/drug (AND) combination as a potential treatment for malignant pleural mesothelioma, PLoS One 8 (2013) e58051, , https://doi.org/10.1371/journal.pone.0058051.
[52] S. Bernichtein, N. Pigat, N. Barry Delongchamps, F. Boutillon, V. Verkarre, P. Camparo, E. Reyes-Gomez, A. Méjean, S.M. Oudard, E.M. Lepicard, M. Viltard, J.C. Souberbielle, G. Friedlander, T. Capiod, V. Goffin, Vitamin D3 prevents calcium-induced progression of early-stage prostate tumors by counteracting TRPC6 and calcium sensing receptor upregulation, Cancer Res. 77 (2) (2017) 355–365, https://doi.org/10.1158/0008-5472.CAN-16-0687.
[53] K. Gioti, R. Tenta, Bioactive natural products against prostate cancer: mechanism of action and autophagic/apoptotic molecular pathways, Planta Med. 81 (7) (2015) 543–562, https://doi.org/10.1055/s-0035-1545845.